Time-Resolved Gas-Phase Kinetic and Quantum Chemical Studies of the Reaction of Silylene with Nitric Oxide

Rosa Becerra

Instituto de Quimica-Fisica "Rocasolano", C.S.I.C., C/Serrano 119, 28006 Madrid, Spain

Sarah-Jane Bowes and J. Steven Ogden

School of Chemistry, University of Southampton, Highfield, Southampton SO17 1BJ, United Kingdom

J. Pat Cannady

Dow Corning Corporation, Mail Stop C01232, 2200 West Salzburg Road, P.O. Box 994, Midland, Michigan 48686-0994

Matthew J. Almond and Robin Walsh*

School of Chemistry, University of Reading, Whiteknights, P.O. Box 224, Reading, RG6 6AD, United Kingdom

Received: September 28, 2004; In Final Form: November 24, 2004

Time-resolved kinetic studies of the reaction of silylene, SiH_2, generated by laser flash photolysis of phenylsilane, have been carried out to obtain rate constants for its bimolecular reaction with NO. The reaction was studied in the gas phase over the pressure range 1−100 Torr in SF_6 bath gas at five temperatures in the range 299−592 K. The second-order rate constants at 10 Torr fitted the Arrhenius equation $\log(k/\mathrm{cm^3\ molecule^{-1}\ s^{-1}}) = (-11.66 \pm 0.01) + (6.20 \pm 0.10\ \mathrm{kJ\ mol^{-1}})/RT\ \ln 10$ The rate constants showed a variation with pressure of a factor of ca. 2 over the available range, almost independent of temperature. The data could not be fitted by RRKM calculations to a simple third body assisted association reaction alone. However, a mechanistic model with an additional (pressure independent) side channel gave a reasonable fit to the data. Ab initio calculations at the G3 level supported a mechanism in which the initial adduct, bent H_2SiNO, can ring close to form cyclo-H_2SiNO, which is partially collisionally stabilized. In addition, bent H_2SiNO can undergo a low barrier isomerization reaction leading, via a sequence of steps, ultimately to dissociation products of which the lowest energy pair are $NH_2 + SiO$. The rate controlling barrier for this latter pathway is only 16 kJ mol^{-1} below the energy of $SiH_2 + NO$. This is consistent with the kinetic findings. A particular outcome of this work is that, despite the pressure dependence and the effects of the secondary barrier (in the side reaction), the initial encounter of SiH_2 with NO occurs at the collision rate. Thus, silylene can be as reactive with odd electron molecules as with many even electron species. Some comparisons are drawn with the reactions of $CH_2 + NO$ and $SiCl_2 + NO$.

Introduction

Silylenes are of importance because they are implicated in the thermal and photochemical breakdown mechanisms of silicon hydrides and organosilanes, as well as being key intermediates in CVD. Time-resolved kinetic studies, carried out in recent years, have shown that the simplest silylene, SiH_2, reacts rapidly with many chemical species.[1,2] Examples of its reactions include Si−H bond insertions and C=C and C≡C π-bond additions.[3] SiH_2 also reacts with many small inorganic molecules such as CO,[4] CO_2,[5] N_2O,[6] H_2O (D_2O),[7−9] and HCl.[10] This class of reactions exhibit significant rate variations, including temperature and pressure dependences, which can be accounted for by a common mechanism involving initial formation of a donor acceptor complex whose behavior, either continuing rearrangement or redissociation back to reactants, determines the overall rate. The kinetic findings in all cases are supported by quantum chemical (ab initio) calculations.[4−10] The reactant molecules in these cases are all closed shell. We turn our attention here to the reaction of SiH_2 with NO (reaction 1), an example of a reaction of silylene with an open shell molecule.

The first and only direct rate study of this reaction was carried out by Chu, Beach, Estes, and Jasinski[11] (CBEJ), who measured rate constants of $(1.5 \pm 0.2) \times 10^{-11}$ cm^3 $molecule^{-1}$ s^{-1} at 1 Torr and $(2.1 \pm 0.2) \times 10^{-11}$ cm^3 $molecule^{-1}$ s^{-1} at 9.5 Torr using helium buffer gas at room temperature. CBEJ[11] pointed out that a weakly pressure dependent reaction implies incomplete collisional stabilization of the vibrationally excited initial SiH_2-NO adduct. Apart from intrinsic interest, NO has long attracted the interests of kineticists because of its use as a radical scavenger. This has been examined previously in silicon hydride systems.[12,13] The analogous reaction of methylene, CH_2, is of interest in combustion chemistry.[14,15] A further interest to us was to compare the behavior toward NO of SiH_2 and $SiCl_2$, which we have studied by end-product analysis.[16] We report here both gas-phase kinetic studies (over a wide range of temperatures and pressures) and quantum chemical (ab initio) calculations of the energy surface. There have been no previous theoretical calculations on this reaction system.

Experimental Section

Equipment, Chemicals, and Method. The apparatus and equipment for these studies have been described in detail previously.[17,18] Only essential and brief details are therefore included here. SiH_2 was produced by the 193 nm flash

10.1021/jp045600p CCC: $30.25
Published on Web 01/25/2005

photolysis of phenylsilane ($PhSiH_3$) using a Coherent Compex 100 exciplex laser. Photolysis pulses were fired into a variable temperature quartz reaction vessel with demountable windows, at right angles to its main axis. SiH_2 concentrations were monitored in real time by means of a Coherent 699-21 single-mode dye laser pumped by an Innova 90-5 argon ion laser and operating with Rhodamine 6G. The monitoring laser beam was multipassed 36 times along the vessel axis, through the reaction zone, to give an effective path length of 1.5 m. A portion of the monitoring beam was split off before entering the vessel for reference purposes. The monitoring laser was tuned to 17 259.50 cm^{-1}, corresponding to a known strong vibration−rotation line[19] in the SiH_2 $\tilde{A}$ ($^1B_1$) ← $\tilde{X}$($^1A_1$) absorption band. Light signals were measured by a dual photodiode/differential amplifier combination, and signal decays were stored in a transient recorder (Datalab DL910) interfaced to a BBC microcomputer. This was used to average the decays of between 5 and 20 photolysis laser shots (at a repetition rate of 0.5 or 1 Hz). The averaged decay traces were processed by fitting the data to an exponential form using a nonlinear least-squares package. This analysis provided the values for first-order rate coefficients, k_{obs}, for removal of SiH_2 in the presence of known partial pressures of substrate gas.

Gas mixtures for photolysis were made up, containing between 2.5 and 6.8 mTorr of $PhSiH_3$, 0−2.4 Torr of NO, and inert diluent (SF_6) up to total pressures of between 1 and 100 Torr. Pressures were measured by capacitance manometers (MKS, Baratron). All gases used in this work were frozen and rigorously pumped to remove any residual air prior to use. $PhSiH_3$ (99.9%) was obtained from Ventron-Alfa (Petrarch). NO(99.5%) was from CK Gas Products. Sulfur hexafluoride, SF_6 (no GC-detectable impurities), was from Cambrian Gases.

Ab Initio Calculations. The electronic structure calculations were performed with the Gaussian 98 software package.[20] All structures were determined by energy minimization at the MP2 = full/6-31G(d) level. Transition state structures were characterized as first-order saddle points by calculation of the Hessian matrix. Stable structures, corresponding to energy minima, were identified by possessing no negative eigenvalues of the Hessian, while transition states were identified by having one and only one negative eigenvalue. The standard Gaussian-3 (G3) compound method[21] was employed to determine final energies for all local minima. For transition states the elements of the G3 method were used, viz. optimization to TS at HF/6-31G(d), frequencies at HF/6-31G(d), optimization to TS at MP2=full/6-31G(d), followed by four single-point energy determinations as in the standard G3 method and combined according to the G3 procedure.[21] The identities of the transition state structures were verified by calculation of intrinsic reaction coordinates[22] (IRC) at the MP2 = full/6-31G(d) or B3LYP/6-31G(d) levels. All local minima and transition state energies were corrected for zero-point energies and converted to enthalpy values at 298.15 K. Where required, harmonic frequencies were obtained from the values calculated at the HF/6-31G(d) level adjusted by the correction factor 0.893 appropriate to this level.[23]

Results

Kinetics. Preliminary experiments established that, for a given reaction mixture, decomposition decay constants, k_{obs}, were not dependent on the exciplex laser energy (50−70 mJ/pulse, routine variation) or number of photolysis laser shots (up to 20 shots). The constancy of k_{obs} (five shot averages) showed no effective depletion of reactants. Higher pressures of precursor were required at the higher temperature because signal intensities decreased with increasing temperature. However, for the purposes of rate constant measurement at a given temperature the $PhSiH_3$ pressure was kept fixed. A series of experiments were carried out at each of five temperatures in the range 299−592 K. At each temperature and at 10 Torr total pressure, at least five runs at different partial pressures of NO were carried out. The results of these experiments are shown in Figure 1, which demonstrates the linear dependence of k_{obs} on [NO], as expected for second-order kinetics. The second-order rate constants at 10 Torr, k_1, obtained by least-squares fitting to these plots, are shown in Table 1. The error limits are single standard deviations and are clearly quite small. Table 1 also includes the values of k^∞ and k°, the rate constants at limiting high and low pressures, respectively, obtained by modeling using RRKM (Rice, Ramsperger, Kassel, Marcus) theory in conjunction with a mechanistic scheme (see below). These have somewhat larger error limits because of the uncertainties of the extrapolation. It is clear that the rate constants decrease with increasing temperature (just as has been found in other similar SiH_2 reactions[1,2,4,6−10]). The Arrhenius plots of all of these rate constants are shown in Figure 2. The fits are reasonably good, and the resulting equations are

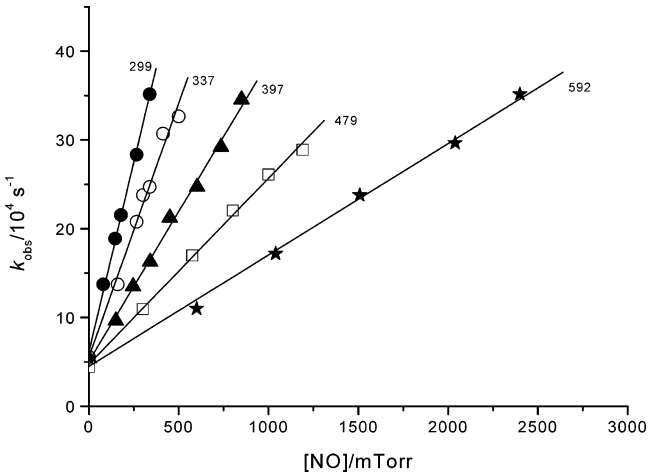

Figure 1. Second-order plots for reaction of SiH_2 + NO at 10 Torr (SF_6): (●) 299, (○) 337, (▲) 397, (□) 479, and (★) 592 K.

TABLE 1: Experimental Second-Order Rate Constants for SiH_2 + NO at 10 Torr (SF_6) and at High and Low Pressures

T/K	k(SF_6, 10 Torr)[a]	k^{∞} [a,b]	k° [a,c]
299	0.265 ± 0.007	4.6 ± 0.9	0.216 ± 0.022
337	0.200 ± 0.010	3.6 ± 0.8	0.159 ± 0.016
397	0.139 ± 0.004	3.2 ± 0.7	0.114 ± 0.011
479	0.104 ± 0.003	1.9 ± 0.6	0.087 ± 0.009
592	0.0769 ± 0.0025	2.6 ± 0.6	0.072 ± 0.007

[a] Units: 10^{-10} cm^3 $molecule^{-1}$ s^{-1}. [b] High-pressure limit (obtained by modeling; see text). [c] Low-pressure limit (obtained by modeling; see text).

$$\text{10 Torr: } \log(k/\text{cm}^3\ \text{molecule}^{-1}\ \text{s}^{-1}) = (-11.66 \pm 0.01) + (6.20 \pm 0.10\ \text{kJ mol}^{-1})/RT \ln 10$$

$$\text{high pressure: } \log(k^{\infty}/\text{cm}^3\ \text{molecule}^{-1}\ \text{s}^{-1}) = (-9.97 \pm 0.18) + (3.44 \pm 1.30\ \text{kJ mol}^{-1})/RT \ln 10$$

$$\text{low pressure: } \log(k^{\circ}/\text{cm}^3\ \text{molecule}^{-1}\ \text{s}^{-1}) = (-11.66 \pm 0.04) + (5.58 \pm 0.32\ \text{kJ mol}^{-1})/RT \ln 10$$

In addition to these experiments, another set of runs were carried out at each temperature. In these, the total pressure (SF_6)

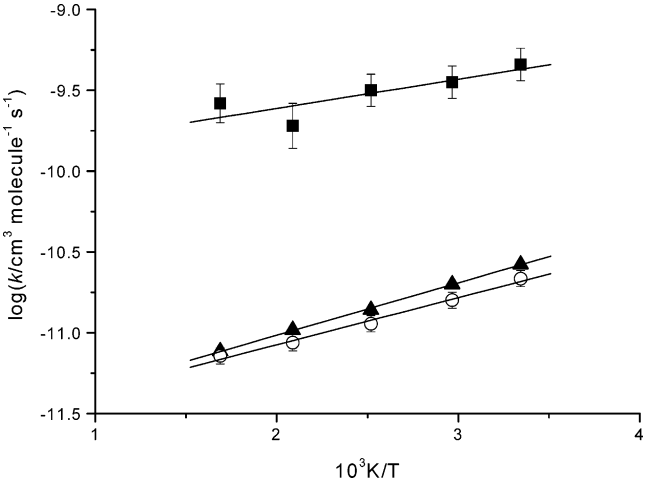

Figure 2. Arrhenius plots of second-order rate constants for SiH_2 + NO: (▲) k_1(10 Torr), (○) $k_1°$, (■) k_1^∞.

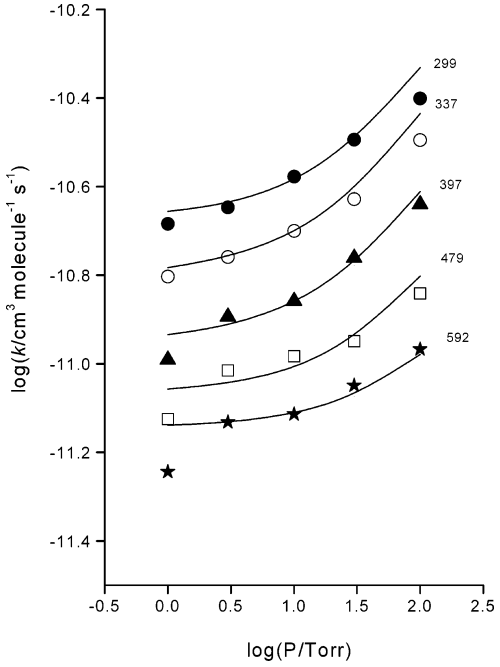

Figure 3. Pressure dependence of second-order rate constants for SiH_2 + NO in the presence of SF_6 at different temperatures. Curves are mechanistic model fits (see text).

was varied in the range 1−100 Torr to test the pressure dependence of the second-order rate constants. The data were obtained in the same way as those at 10 Torr, although since second-order behavior had been established at 10 Torr, only three or four NO substrate partial pressures were tried at each total pressure. The rate constant for reaction of SiH_2 with precursor (intercept point on the second-order plots) was found to be pressure independent. The pressure range was limited by practical considerations. Above ca. 100 Torr transient signals became too small, and below 1 Torr, pressure measurement uncertainties became significant. The results from these experiments are plotted in Figure 3, which clearly demonstrates the pressure dependence of the rate constants at each temperature. For convenience, log−log plots are used. The uncertainties are not shown in the figures, but they are estimated at ca. ±10%.

From examination of Figure 3 several points are evident. Rate constants decrease with increasing temperature at all pressures. At each temperature the rate constants increase with increasing pressure to a very similar extent. Although these effects are qualitatively characteristic of a third-body-mediated association reaction, normally such reactions show stronger pressure dependences at the higher temperatures. To investigate this and also to be able to extrapolate the data to the high-pressure limit, k^∞, we have carried out RRKM modeling calculations,[24] as described in the next section.

RRKM Calculations. The pressure dependence of an association reaction corresponds exactly to that of the reverse unimolecular dissociation process, providing there are no other perturbing reaction channels. The ab initio calculations (see next section) suggest that there are other channels. We have encountered this situation in studies of GeH_2 reaction systems.[25,26] Thus, as previously, we began by modeling the association reaction assuming there were no side reactions and then proceeded by making allowance for such a channel.

(i) Scheme without Side Reactions. The ab initio calculations suggest that while the initial adduct of SiH_2 + NO is the bent H_2SiNO isomer, this can very easily close to the cyclic-H_2SiNO form, which is significantly more stable. This is shown in Scheme 1. Thus, the process modeled by RRKM corresponds

SCHEME 1

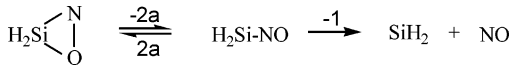

to the decomposition of cyclo-H_2SiNO via a transition state, TS1, appropriate to dissociation of bent H_2SiNO. The RRKM calculations were carried out in combination with a collisional deactivation model (also called the master equation method), the details of which are given below. Since experimental details of the structures and vibrational wavenumbers of the species of interest here are not available, we have taken information from the output of the theoretical calculations where possible and made empirical adjustments where necessary.

TS1 was not identified by the ab initio calculations, and therefore its vibrational assignment was carried out as follows. The decomposition A factor, A_D, is required (in this case equal to $A_{-2a}A_{-1}/A_{2a}$). A_D is obtained via the microscopic reversibility relationship, $\ln(A_D/A_A) = \Delta S°/R$, where $\Delta S°$ is the overall entropy change and A_A the experimental, high-pressure-limiting A factor for association, i.e., A_1. The value for $\Delta S°$ (for the overall reaction, −2a, 2a, −1) was obtained as + 147.1 J K^{-1} mol^{-1} at 298 K from the ab initio calculations. The value for A_1 was not so easily obtained since the extrapolation of the experimental data to the high-pressure limit is not straightforward. We therefore adopted a trial value of $A_1 = 1 \times 10^{-10}$ cm^3 $molecule^{-1}$ s^{-1} by analogy with the measured values for several encounter-controlled SiH_2 reactions.[17,27−32] This gave (at 298 K) $A_D = 10^{16.61}$ s^{-1}. The ab initio calculations do not provide the temperature dependence of $\Delta S°$ which will give rise to a slight temperature dependence of A_D. For most SiH_2 reactions, transition states are variational in the sense that A_D values decrease with temperature. We therefore estimated the decrease in A_D with temperature, which corresponded to previous experience with other reactions.[17,27−29,31,32] The A_D values at the temperatures of interest are shown in Table 2. The values of A_D were then used as the basis for adjustment of the vibrational wavenumbers of the bent H_2SiNO molecule (obtained from the ab initio calculations) to obtain those of the

TABLE 2: Estimated *A* Factors for Cyclo-H_2SiNO Decomposition

T/K	299	337	397	479	592
$\log(A_D/s^{-1})$	16.61	16.51	16.38	16.25	16.11

TABLE 3: Molecular and Transition State Parameters for RRKM Calculations for Decomposition of the Cyclo-H_2SiNO[a]

parameter	cyclo-H_2SiNO	bent H_2SiNO	TS1
$\tilde{\nu}$/cm^{-1}	2217	2167	2167
	2208	2127	2127
	1030	1327	1800
	949	901	901
	778	664	110
	734	623	100
	658	591	rxn coord
	642	301	49
	505	187	30
A/s^{-1}			4.07×10^{16}
E_0/kJ mol^{-1}			163.3
Z/10^{-10} cm^3 molecule^{-1} s^{-1}			4.55

[a] Calculated at 299 K.

TABLE 4: Temperature-Dependent Parameters Used in RRKM Calculations for Cyclo-H_2SiNO Decomposition

	T/K				
parameter	299	337	397	479	592
$\tilde{\nu}$(TS)/cm^{-1}	110	120	120	125	130
	100	110	111	114	115
	49	49	52	55	55
	30	30	34	35	37
$\Delta H°$/kJ mol^{-1}	177.0	177.0	177.0	177.0	177.0
E_0/kJ mol^{-1}	163.3	162.7	161.9	161.0	159.9
Z_{LJ}/10^{-10} cm^3 molecule^{-1} s^{-1}	4.55	4.61	4.74	4.87	5.06

activated complex (TS1) at each temperature of decomposition. This was done by reducing those for the Si−N═O bending modes and SiH_2 wagging and rocking modes until the entropy of activation, $\Delta S^{‡}$, and A factor were matched at each temperature. The Si−N stretch was taken as the reaction coordinate. The full details of this are shown in Table 3 for TS1 at 299 K. For the temperature-dependent parameters, such as the transitional vibrational modes, the values are given in Table 4. It should be noted that although bent H_2SiNO was used as the basis for estimating $S°$(TS1), $\Delta S^{‡}$ corresponds to $S°$(TS1) − $S°$(cyclo-H_2SiNO).

We have assumed, as previously,[31,32] that geometry changes between reactant and transition states do not lead to significant effects. In modeling the collisional deactivation process, we have used a weak collisional (stepladder) model[24] because there is considerable evidence against the strong collision assumption.[33] The average energy removal parameter, $\langle\Delta E\rangle_{down}$, which determines the collision efficiency, was taken as 12.0 kJ mol^{-1} (1000 cm^{-1}).

The initial value for the critical energy, E_0, was obtained from the ab initio calculation for $\Delta H°$ (for reaction −2a, 2a, −1) by subtraction of the thermal energy from E_a, obtained via $E_a = \Delta H° + E_{-a} - RT$. Initially, E_{-a} was set at −4.2 kJ mol^{-1} by comparison with earlier studies,[27−32] giving E_0 as 162.8 kJ mol^{-1} at 299 K. When we carried out the first set of calculations, it became quickly apparent that the predicted pressure dependence was far greater than that observed (at each temperature). These results were well outside any small uncertainties of the model (assumptions of collision efficiencies, vibrational assignments, possible incorporation of active rotations, etc.). We thus decided to investigate the effect of changing E_0. Figure 4 shows the results of these calculations at 299 K for a set of values of E_0 ranging from 163 up to 293 kJ mol^{-1}. It is clear that changing E_0 does not improve the fit; it merely shifts the curves. Even if our assumptions about A_1 and E_{-a} were wrong, these curves could not be matched with experiment. The lack of fit is even

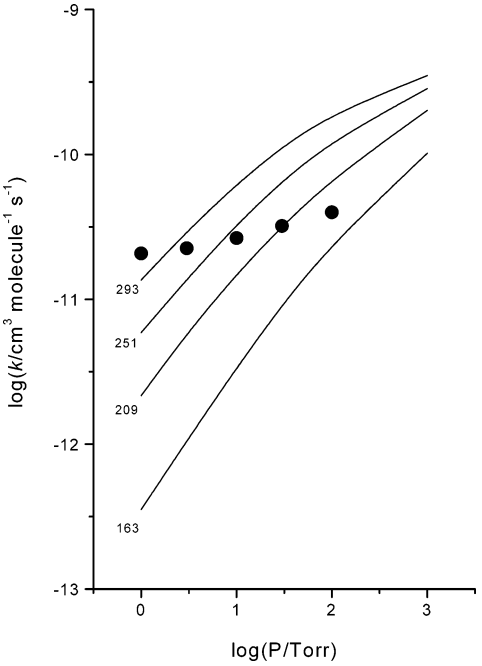

Figure 4. RRKM theoretical curves for SiH_2 + NO → cyclo-H_2SiNO at 299 K. The different curves are derived for different values of the critical energy, E_0/kJ mol^{-1}, as indicated. ● represent experimental points.

greater at higher temperatures. Thus, uncertainty in the ab initio results for E_0 cannot be the cause of the discrepancy, and the explanation for the lack of fit must lie elsewhere. Since pressure dependences only occur for reversible processes, it is clear that another, irreversible, reaction channel must be effectively competing to remove one of the vibrationally excited intermediates prior to stabilization.

(ii) Scheme with Side Reaction. As found in other reaction systems of SiH_2,[10,27] the initial product (or complex) is capable of further reaction as confirmed by the ab initio calculations (see below). We therefore adapted the RRKM modeling to Scheme 2. In this scheme, I* may be considered as the

SCHEME 2

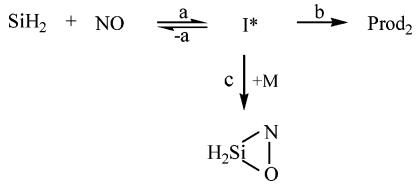

vibrationally excited bent H_2SiNO species. $Prod_2$ is one (or more) of the species accessible on the potential energy surface (see next section). Steps a and −a correspond to 1 and −1 of Scheme 1. Step b corresponds to reaction via TS2b on the ab initio surface. Step c corresponds to stabilization of cyclo-H_2-SiNO* in dynamic steady state with I* via steps 2a and −2a. The modeling of such a scheme is more complicated than the simple association. Stationary state treatment of I* gives the rate equation

$$k_{obs} = k_a[NO]\frac{k_b + k_c[SF_6]}{k_{-a} + k_b + k_c[SF_6]} \qquad (X)$$

Equation X gives for the second-order rate constant, k_1 (=k_{obs}/[NO]), the values k_a (= k^{∞}) at the high-pressure limit and k_a/(1 + k_{-a}/k_b) (= $k°$) at the low-pressure limit. The modeling of the

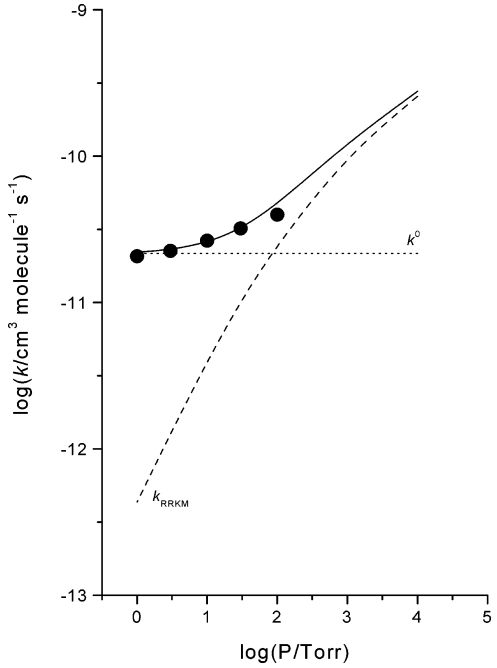

Figure 5. Pressure dependence of second-order rate constants for SiH_2 + NO in the presence of SF_6 at 299 K. Solid curve shows model fit. Dotted and dashed curves show contributions of pressure-independent ($k°$) and pressure-dependent (k_{RRKM}) contributions.

data was done as follows. At each temperature the measured k_1 value at the lowest pressure (1 Torr) was taken as the initial fix for $k°$ since the RRKM calculated contribution was very small at 1 Torr. This value was then used to obtain the pressure-dependent contributions to the rate constants $k_1 - k°$ at other pressures. These were then refitted at each temperature by the RRKM calculations, which were refined using the vibrational assignments consistent with the variational TS shown in Table 4. This fitting enabled extrapolation to the high-pressure limit to give the values for k_a ($= k^\infty$). The calculated pressure-dependent rate constants were then used to refine the low-pressure limiting values, $k°$, by using weighted values for $k_1 - k_{RRKM}$ at each temperature. After a further cycle final values were obtained for the high- and low-pressure rate constants. These are shown in Table 1. They were then used to model the pressure dependence curves for comparison with experiment at each temperature. These curves are shown in Figure 3. An illustration of how the individual pressure-dependent and pressure-independent contributions to the rate constants at 299 K are combined is shown in Figure 5. Similar plots were obtained at the other temperatures.

Ab Initio Calculations. Possible species on the SiH_2NO potential energy surface (PES) were explored in detail at the G3 level of theory. Apart from the reactant species SiH_2 + NO, 18 isomeric five-atomic molecules (stable minima) were found as well as 21 possible pairs of dissociation fragments. In addition, 14 transition states were identified, not including those for dissociation processes. Because of the complexity of possible reaction mechanisms, the description of these results is divided into two parts, viz. (i) species involved in energetically favorable (i.e., probable) pathways and (ii) species involved in energetically unfavorable (but possible) pathways. A third category, including species with unfavorable energies or favorable energies but not linked to the identified pathways, is listed in the Appendix.

(i) Species Involved in Energetically Favorable Pathways. These stable species and the transition states linking them are shown in the potential energy surface in Figure 6 and their structures in Figure 7. Total energies and relative enthalpy values are listed in Table 5. When SiH_2 and NO initially combine, they can form both O- and N-bonded adducts. The N-bonded species is the more stable and exists in a bent anti-configuration with *r*- and *l*-handed forms (C_1 point group). The pyramidal configuration at Si indicates a silicon-centered free radical. The transition state for formation of bent H_2SiNO, although not found in these calculations, was designated TS1 for consistency with the Schemes 1 and 2. Bent H_2SiNO can ring close via a low-energy transition state, TS2a, to form cyclo-H_2SiNO (C_s point group), an N-centered free radical. We were unable to find any further direct or onward process from cyclo-H_2SiNO to other species. However, bent H_2SiNO can undergo a relatively low-energy 1,2 H-shift process (Si to N) via TS2b to give the HSi−NH−O species, best described as a silylene-substituted nitroxide radical. This species then ring closes via TS3a, another low-energy transition state, to form cyclo-HSiNHO (C_1 point group), an Si-centered free radical. This ring then opens by N−O bond fission, via a further low-energy transition state, TS4a, to form HN(Si═O)H, a silanonyl-substituted amino radical. The gain in stability here is substantial, due in part to the strength

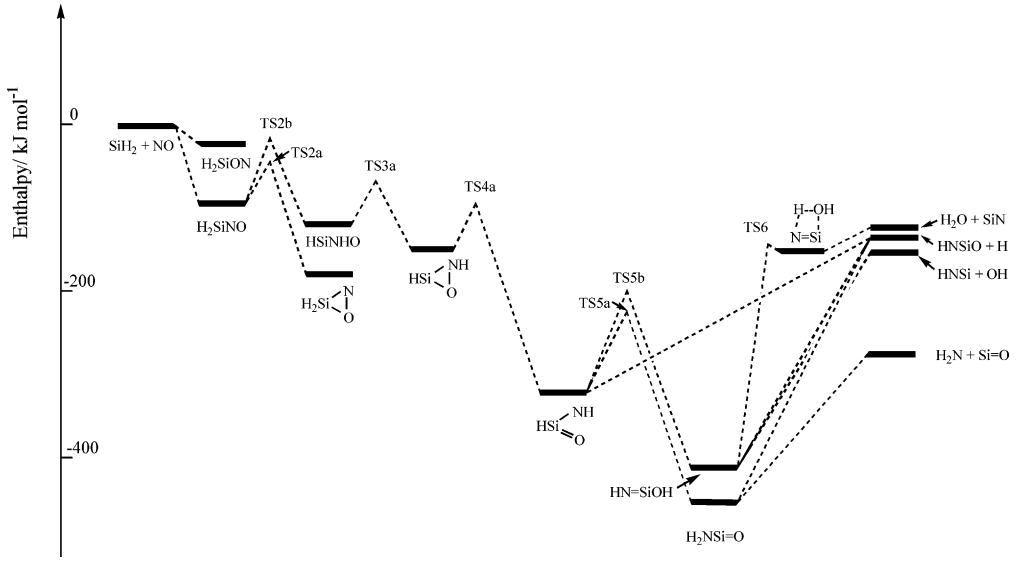

Figure 6. Potential energy (enthalpy) surface showing the most likely species involved in the reaction of SiH_2 + NO. All enthalpies (kJ mol^{-1}) are calculated at the ab initio G3 level.

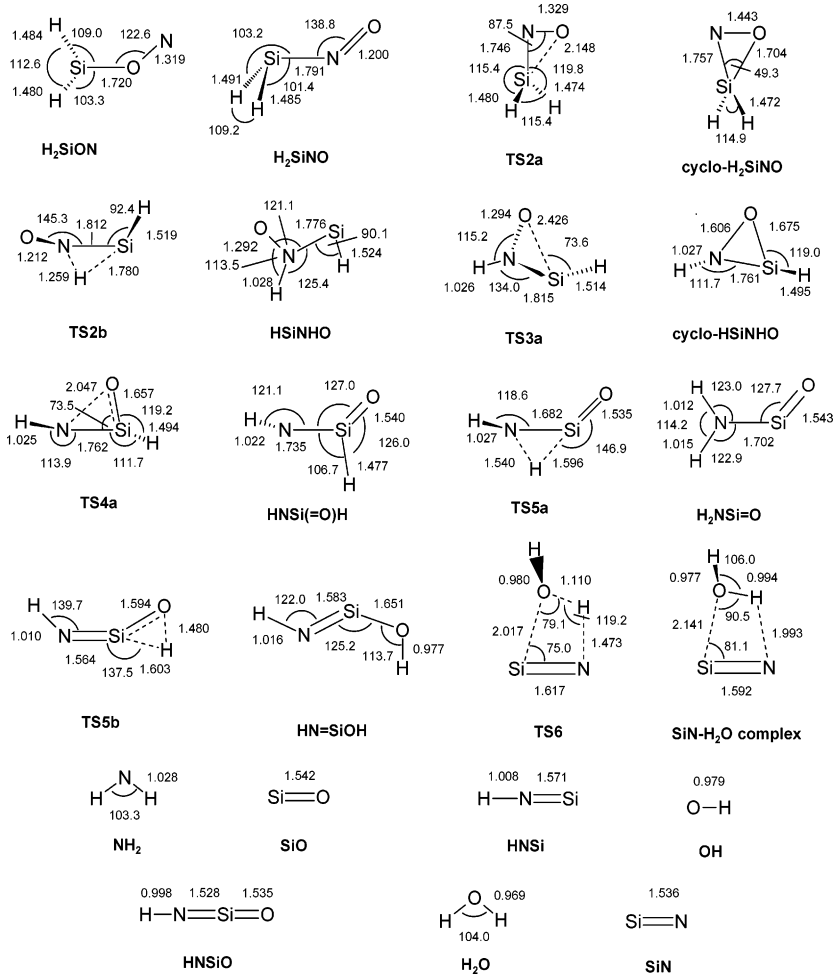

Figure 7. Ab initio MP2=full/6-31G(d) calculated geometries of local minimum structures and transition states of probable involvement in the SiH_2 + NO reaction. Selected distances are given in angstroms and angles in degrees.

TABLE 5: Ab Initio (G3) Enthalpies for SiH_2NO Species of Probable Involvement in the Reaction of SiH_2 with NO

molecular species	energy/hartree	relative energy/kJ mol^{-1}
SiH_2 + NO	−420.284314	0
H_2SiON	−420.294598	−27
H_2SiNO	−420.320622	−95
TS2a	−420.300893	−44
cyclo-H_2SiNO	−420.351578	−177
TS2b	−420.290549	−16
HSiNHO	−420.329962	−120
TS3a	−420.310561	−69
cyclo-HSiNHO	−420.341117	−149
TS4a	−420.320558	−95
HNSi(=O)H	−420.405784	−319
TS5a	−420.368671	−221
H_2NSi=O	−420.440674	−411
NH_2 + SiO	−420.386782	−269
TS5b	−420.359192	−197
HN=SiOH	−420.454529	−447
TS6	−420.339169	−144
SiN··H_2O complex	−420.342459	−153
H_2O + SiN	−420.333012	−128
HNSiO + H	−420.336326	−137
HNSi + OH	−420.343539	−155

of the Si=O double bond. This molecule can isomerize by 1,2 H-shift either from Si to N (via TS5a) to make H_2NSi=O, the aminosilanonyl free radical, or from Si to O (via TS5b) to make HN=SiOH, the hydroxy(imino-)silyl radical. The last three molecules all possess dissociation pathways, the lowest energy of which gives NH_2 + Si=O. However, the high overall energy release in this system means that the product pairs HNSi + OH (from HN=SiOH), HNSiO + H (from HNSi(=O)H, HN=SiOH, and H_2NSi=O) and H_2O + SiN (from HN=SiOH) are all energetically feasible. We have not calculated transition state structures for these dissociation processes, except in the case of H_2NSi=O to NH_2 + Si=O. Here the TS enthalpy (−288 kJ mol^{-1}) apparently lies below that of the dissociation products. On the basis of this, we do not expect any of the other dissociations to involve serious additional energy barriers.

This complicated pathway thus suggests that the mechanistically controlling intermediate is the vibrationally excited, bent H_2SiNO molecule. Because of the availability of pathways through both TS2a and TS2b, this species can lead partially to cyclo-H_2SiNO and partially, through a series of sequential steps, to dissociation products of which NH_2 + Si=O look to be most likely (or predominant). The ratio of the two channels will depend on the extent of stabilization of cyclo-H_2SiNO and will thus be pressure dependent.

(ii) Species Involved in Energetically Unfavorable Pathways. These stable species and the transition states linking them are shown in the potential energy surface in Figure 8 and their structures in Figure 9. Total energies and relative enthalpy values are listed in Table 6. The chief feature of these species and of the scheme of Figure 8 is that, whereas the stable species all have energies below that of SiH_2 + NO, one transition state in each branch of the pathway here has a positive energy value (i.e., too high to be surmounted). Although these pathways are apparently ruled out by a single high barrier, their importance is that they appear plausible, and any error in the accuracy of

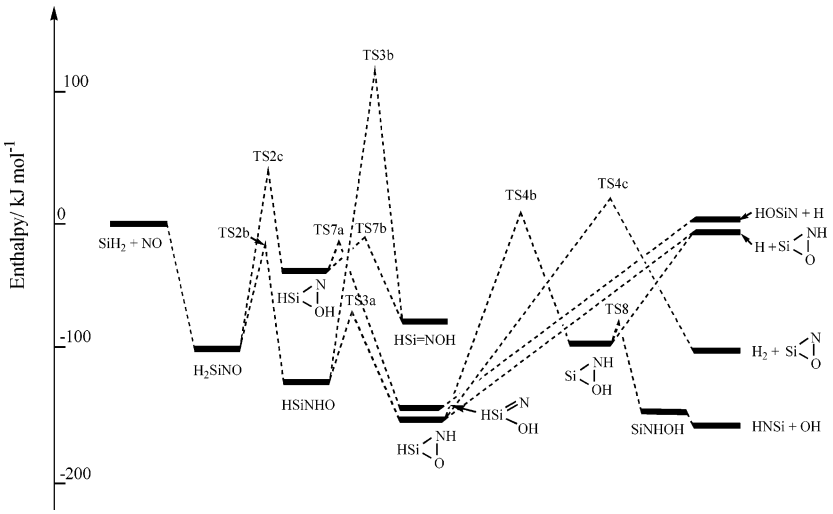

Figure 8. Potential energy (enthalpy) surface showing the less likely species involved in the reaction of SiH_2 + NO. All enthalpies (kJ mol^{-1}) are calculated at the ab initio G3 level.

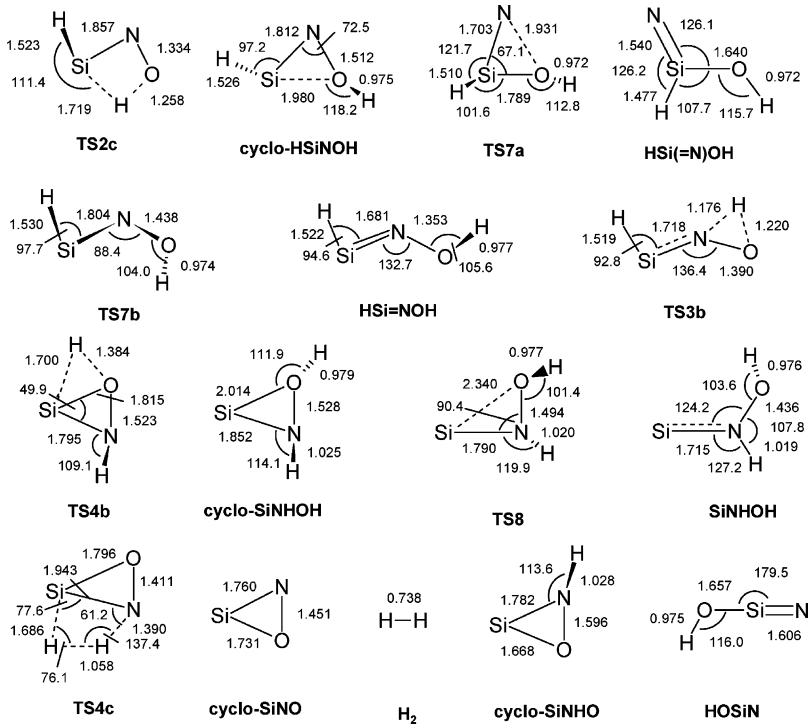

Figure 9. Ab initio MP2=full/6-31G(d) calculated geometries of local minimum structures and transition states of possible involvement in the SiH_2 + NO reaction. Selected distances are given in angstroms and angles in degrees.

the calculations could mean that their consideration is still required. Additionally, they provide a comparison with their analogues in the CH_2NO system.[14]

These pathways are all shown starting from bent H_2SiNO. The first of these, via TS2c, involves a 1,3 H-shift simultaneous with ring closure to form cyclo-HSiNOH, which may be regarded as another silylene-substituted N-centered radical, stabilized by internal lone pair donation from O to Si. TS2c is 44 kJ mol^{-1} above SiH_2 + NO, which should rule this pathway out. Cyclo-HSiNOH, however, has two low-energy ring-opening pathways, the first via TS7a, an N−O bond fission process, and the second via TS7b, an Si−O bond fission. These pathways yield respectively HSi(=N)OH, the hydroxysilaiminyl radical, and HSi=NOH, an Si-centered silaoxime radical. Whereas HSi=NOH appears to have no low-energy dissociation pathway, HSi(=N)OH can dissociate to HOSiN + H which, at 3 kJ mol^{-1}, is only marginally above threshold.

TABLE 6: Ab Initio (G3) Enthalpies for SiH_2NO Species of Possible Involvement in the Reaction of SiH_2 with NO

molecular species	energy/hartree	relative energy/ kJ mol^{-1}
TS2c	−420.267522	+44
cyclo-HSiNOH	−420.297651	−35
TS7a	−420.289693	−14
HSi(=N)OH	−420.338317	−142
HOSiN + H	−420.283136	+3
TS7b	−420.288431	−11
HSi=NOH	−420.315426	−73
TS3b	−420.241805	+112
TS4b	−420.280802	+9
cyclo-SiNHOH	−420.319064	−91
TS8	−420.313375	−76
SiNHOH	−420.338843	−143
TS4c	−420.276564	+20
cyclo-SiNO + H_2	−420.320759	−96
cyclo-SiNHO + H	−420.287870	−9

The second pathway from bent H_2SiNO proceeds to HSiNHO (via TS2b, as before). At this point a bifurcation of the surface, via TS3b, involving a 1,2 H-shift from N to O leads to HSi═NOH, the same product formed via TS7b. However, this route via TS3b, at 112 kJ mol^{-1}, seems rather unlikely. If the system proceeds via TS3a, as before, to cyclo-HSiNHO, then two further possibilities open up. The first, via TS4b, involves a 1,2 H-shift from Si to O leading to cyclo-SiNHOH, which may be regard as an N-substituted silylidyne stabilized by an internal lone pair donation from O to Si. TS4b is only 9 kJ mol^{-1} above SiH_2 + NO. Cyclo-SiNHOH then ring opens via TS8 by Si−O bond fission to the bent form of SiNHOH, which gains in stability through relief of ring strain. This species is barely stable, however, since it has a downhill dissociation pathway to HNSi + OH. The other pathway from cyclo-HSiNHO, via TS4c, leads to cyclo-SiNO + H_2. TS4c, at 20 kJ mol^{-1}, is also only slightly above SiH_2 + NO. Both cyclo-HSiNHO and cyclo-SiNHOH can dissociate to H + cyclo-SiNHO. It is interesting to note that, of the eight possible forms of "HSiNO" which might be formed by H atom loss from any of the "H_2SiNO" species, only two, viz. HNSiO and cyclo-SiNHO, are energetically accessible from SiH_2 + NO.

The remaining species are listed and discussed in the Appendix.

Discussion

General Comments and Rate Constant Comparisons. The main experimental purpose of the present work was to study the temperature and pressure dependence of the rate constants for the reaction of SiH_2 with NO. This has been accomplished and the reaction found to have a moderately high *A* factor and small negative activation energy. This is discussed in more detail below. Comparison with the previous study of CBEJ[11] shows that our value of the room temperature rate constant ((2.65 ± 0.07) × 10^{-11} cm^3 molecule^{-1} s^{-1}) in 10 Torr of SF_6, shown in Table 1, is slightly higher than theirs ((2.1 ± 0.2) × 10^{-11} cm^3 molecule^{-1} s^{-1}) in 9.5 Torr of He. There is a similar small difference between values at 1 Torr total pressure. Given that SF_6 is a more efficient collision partner than He and the reaction is pressure dependent, these differences are reasonable and suggest no serious discrepancy between our results and those of CBEJ.[11] In an earlier, but not time-resolved, study of SiH_2 with NO, Dohmaru and Lampe[13] used the IRMPD (infrared multiple photon decomposition) method to generate SiH_2 from SiH_4. They interpreted their results to show that SiH_2 apparently reacted ca. 4.4 times faster with NO than with SiH_4. Comparison of the results obtained here with our own direct study of SiH_2 + SiH_4[17] suggests that, on the contrary, reaction of SiH_2 with NO is ca. 10 times slower than with SiH_4. It seems likely to us that in the IRMPD system complexities of mechanism make rate constant comparisons difficult. Sandhu et al.[34] obtained a rate constant of (2.65 ± 0.17) × 10^{-12} cm^3 molecule^{-1} s^{-1} for the reaction of $SiCl_2$ + NO. Experiments were carried out in 100 Torr of argon, but no pressure dependence was reported. The order of magnitude slower reaction for $SiCl_2$ compared with SiH_2 is consistent with general reduced reactivity of $SiCl_2$ compared with SiH_2.[35]

The negative activation energy found in this study, as in previous SiH_2 studies,[4,6−10,17,27−32,36,37] could be interpreted either as evidence of involvement of an intermediate complex[7−10,17,30−32,36] or as arising from angular momentum effects in a typical radical recombination process.[27−29,37] The situation is further complicated because the pressure dependence found is evidence for a third body assisted association reaction not at its high-pressure limit under experimental conditions. From the kinetic information alone, it is not possible to determine whether an intermediate complex is involved (in step 1). However, the ab initio calculations taken in conjunction with the RRKM modeling throw considerable further light on the mechanism. These are described in the next section.

RRKM Calculations, ab Initio Calculations, and the Mechanism. The idea of combination of SiH_2 with NO to form a simple adduct in the initial step is borne out by the ab initio calculations. The Si−O bonded species, H_2SiON, favored by Dohmaru and Lampe,[13] is found to be too weakly bound to play a role in the mechanism. The kinetic results fit best with formation of the Si−N bonded species, H_2SiNO (step 1), which can then ring close to cyclo-H_2SiNO (step 2a), in line with the ab initio results. Our test of this mechanism as a third body assisted association using RRKM theory, however, reveals that it is insufficient to explain the results. No sensible combination of TS structure and critical energy for this combination mechanism alone can reproduce the observed pressure dependence. The height of the barrier TS2a, at 44 kJ mol^{-1} below SiH_2 + NO, provides no hindrance to cyclization of H_2SiNO. However, we have found that a mechanism in which a parallel irreversible rearrangement of H_2SiNO also occurs can provide a fit to the data. The comparison in Figure 3 between experiment and the mechanistic model prediction shows reasonable agreement, except possibly at the lowest pressures (1 Torr). While errors are often largest at 1 Torr, it is possible that there is a small pressure dependence to $k°$ since weak collisions can alter the populations of vibrationally excited H_2SiNO species, which will affect the partition of molecules proceeding via TS2a and TS2b. This effect, while not expected to be large, was not taken into account in our calculations.

The measured Arrhenius parameters for the reaction provide added support for the mechanism. Because of the pressure dependence, the values obtained experimentally at 10 Torr (log(A/cm^3 molecule^{-1} s^{-1}) = −11.66 and E_a = −6.20 kJ mol^{-1}) are much closer to the low-pressure limiting values (log($A°$/cm^3 molecule^{-1} s^{-1}) = −11.66 and $E_a°$ = −5.58 kJ mol^{-1}) than the high-pressure ones (log(A^∞/cm^3 molecule^{-1} s^{-1}) = −9.97 and E_a^∞ = −3.44 kJ mol^{-1}). The low-pressure limiting values are however not those of a purely thermal process. Nevertheless, if this corresponds to a bottleneck partly controlled by a tight transition state, the parameters should reflect this. The ab initio calculations show that at −16 kJ mol^{-1} TS2b is not far below the reaction energy threshold and therefore should exert some effect. (We have discussed the effects of secondary bottlenecks in a recent paper.[10]) From the ab initio calculations we can obtain an estimate of the entropy of TS2b of 271 J K^{-1} mol^{-1} via the calculated structure and vibrational wavenumbers. We can then use the transition state theory expression (A = $e^2(kT/h)$ exp($\Delta S^‡/R$))[38] to calculate a log(A/cm^3 molecule^{-1} s^{-1}) value of −12.71 (using also calculated entropies for SiH_2 and NO). Although the measured value for log($A°$/cm^3 molecule^{-1} s^{-1}) is not as low as this, it is only 1 order of magnitude greater, whereas it is smaller by a factor of $10^{1.7}$ than A^∞, the high-pressure A factor corresponding to the loose TS for actual association of SiH_2 + NO. Thus, the considerable tightening of the transition state associated with the pressure-independent pathway does suggest the influence of a mechanistic route via a transition state of the type corresponding to TS2b. It is worth noting also that the data fit produced a high-pressure A factor (log(A^∞/cm^3 molecule^{-1} s^{-1}) = −9.97) in very good agreement with the trial value (−10.00). This reinforces the idea that, like many other SiH_2 reactions,[17,27−32,36,37] the reaction with NO is

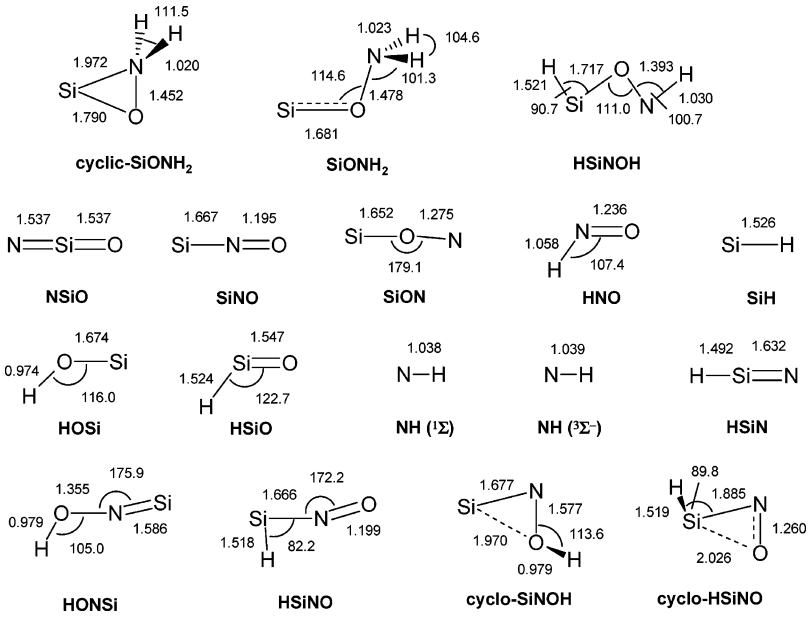

Figure 10. Ab initio MP2=full/6-31G(d) calculated geometries of some miscellaneous local minimum structures, including dissociation fragments, on the SiH_2NO energy surface. Selected distances are given in angstroms and angles in degrees.

occurring at the collisionally controlled rate. Using the Lennard-Jones formula[39] in conjunction with the necessary parameters,[30,40] the collision number, Z_{LJ}, for $SiH_2 + NO$ is calculated to be 3.68×10^{-10} cm^3 molecule^{-1} s^{-1} at 298 K. Comparison with the value of k^∞ in Table 1 shows agreement with Z_{LJ} (within experimental error). Thus, despite its odd electron character, NO is merely another reactive substrate like many others (e.g., SiH_4,[17] GeH_4,[30] C_2H_4,[28] C_2H_2,[27] Me_2CO[31]), able to satisfy the extreme electrophilic demands of SiH_2 only by reaction on every encounter. It does not seem to matter whether SiH_2 is offered one electron or two!

The ab initio calculations are completely consistent with this mechanistic model and furthermore provide some insight into the route followed by the system after passage across TS2b. Through a reasonable series of steps involving 1,2 H-shifts, ring closures, and bond breakings, the system can reach a number of pairs of atomic and molecular fragments, the most likely of which would appear to be $NH_2 + SiO$. The other possible product pairs (HNSi + OH, HNSiO + H, and H_2O + SiN), while they are energetically accessible, are likely to be formed much more slowly, and therefore in lower yields, because their higher energies imply lower values for their microcanonical formation rate constants. The investigation of these products is beyond the scope of the present study.

While there is no previous theoretical study of this reaction system, there has been an ab initio and DFT study of the analogous energy surface of $CH_2 + NO$ by Fikri et al.[14] Calculations at the B3LYP/6-311G(d,p) and G2 levels showed the most likely reaction products to be H + HCNO, with a smaller likelihood of forming HCN + OH. The calculations agreed with their experimental investigation[14] of CH_2 ($^3B_1$) with NO. As can be seen in the Appendix, the analogous products, H + HSiNO and HSiN + OH, are too high in energy to be formed in the present system. This is not too surprising since it reflects the reversal of stabilities of HNSi and HSiN and of HNSiO and HSiNO compared to their carbon counterparts. This arises for the well-known reasons (i) that Si forms weaker multiple bonds than C, (ii) that Si in the divalent state is stabilized, and (iii) Si prefers to be between two electronegative atoms (where possible). There is one respect, however, in which the CH_2NO and SiH_2NO systems are similar. In the CH_2 + NO system the product pair, $NH_2 + CO$, is the lowest in energy, analogous to the result from the present system. Non observation of $NH_2 + CO$ suggests that one or more of the barriers on the energy surface for their formation must be too high. Although Fikri et al.[14] did not calculate the energy barrier for this pathway in the CH_2 + NO system, more elaborate calculations by Shapley and Bacskay[41,42] of the CH_2NO energy surface suggest that the lowest energy route from CH_2NO to NH_2CO (the precursor to $NH_2 + CO$) has to pass a barrier marginally higher in energy than $CH_2(^3B_1)$ + NO. It seems as though theory and experiment are in agreement on this point although there have been earlier claims that NH_2 was a product of CH_2 + NO.[43] There are many detailed differences between the CH_2NO and SiH_2NO energy surfaces, but they mostly appear to reflect the bonding differences between C and Si referred to above and therefore are not discussed further here.

We recently carried out some calculations (G3) of the energy surface for $SiCl_2 + NO$.[16] Although less extensive that those reported here for $SiH_2 + NO$, they nevertheless showed that the key intermediate was cyclo-Cl_2SiNO. This species appeared to be sufficiently stable under reaction conditions to undergo further reaction with another NO molecule to produce the observed products Cl_2 and N_2O. The conditions of these latter experiments (high-temperature pyrolysis source of $SiCl_2$ and flow system with mass spectrometric detection) are, however, far removed from those of the present study. At the low partial pressures of NO and high dilutions with SF_6, secondary reactions of cyclo-H_2SiNO with NO would be unlikely to perturb the kinetics reported here.

Acknowledgment. We are grateful to Dow Corning Corporation for financial support of this work. R.B. also thanks the Spanish DGI for support under Project BQU2002-03381. We thank Mark Blitz for a prepublication copy of his CH_2 + NO paper.

Appendix

This contains details of the ab initio results on two further groups of SiH_2NO species, viz. those with favorable energies (relative to $SiH_2 + NO$), but which we were unable to link to other species on the surface, and those with unfavorable energies. The structures of these species are shown in Figure 10,

TABLE 7: Ab Initio (G3) Enthalpies for SiH_2NO Species Not Clearly Involved in the Reaction of SiH_2 with NO

molecular species	energy/hartree	relative energy/kJ mol^{-1}
cyclo-$SiONH_2$	−420.349692	−172
$SiONH_2$	−420.345695	−161
HSiNOH	−420.325019	−107
SiNO + H_2	−420.321032	−96
NSiO + H_2	−420.267117	+45
SiON + H_2	−420.264601	+52
SiOH + ^{3}NH	−420.288316	−11
SiOH + ^{1}NH	−420.221762	+164
HSiO + ^{3}NH	−420.274339	+26
HSiO + ^{1}NH	−420.207785	+201
HNO + SiH	−420.238440	+120
HSiN + OH	−420.238412	+121
HONSi + H	−420.268981	+40
HSiNO + H	−420.245689	+101
cyclo-SiNOH + H	−420.245835	+101
cyclo-HSiNO + H	−420.217613	+175

and their total energies and relative enthalpies are listed in Table 7. The five-atomic species (HSiONH, $SiONH_2$, and cyclo-$SiONH_2$) may have connections to other isomers, but we did not find them. Although the energy of the dissociated pair SiNO + H_2 is favorable, we could not find a transition state linking it to bent or cyclic H_2SiNO. The dissociated pair, SiOH + ^{3}NH, could be linked to the species in Figure 6, but in view of its only small energy gain relative to SiH_2 + NO, in comparison with other pathways, we chose to list it here.

References and Notes

(1) Jasinski, J. M.; Becerra, R.; Walsh, R. *Chem. Rev.* **1995**, *95*, 1203.

(2) Becerra, R.; Walsh, R. Kinetics & mechanisms of silylene reactions: A prototype for gas-phase acid/base chemistry. In *Research in Chemical Kinetics*; Compton, R. G., Hancock, G., Eds.; Elsevier: Amsterdam, 1995; Vol. 3, p 263.

(3) Gaspar, P. P.; West, R. Silylenes. In *The Chemistry of Organic Silicon Compounds*; Rappoport, Z., Apeloig, Y., Eds.; Wiley: Chichester, 1998; Vol. 2, Chapter 43, p 2463.

(4) Becerra, R.; Cannady, J. P.; Walsh, R. *J. Phys. Chem. A* **2001**, *105*, 1897.

(5) Becerra, R.; Cannady, J. P.; Walsh, R. *J. Phys. Chem. A* **2002**, *106*, 4922.

(6) Becerra, R.; Frey, H. M.; Mason, B. P.; Walsh, R. *Chem. Phys. Lett.* **1991**, *185*, 415.

(7) Alexander, U. N.; King, K. D.; Lawrance, W. D. *J. Phys. Chem. A* **2002**, *106*, 973.

(8) Becerra, R.; Cannady, J. P.; Walsh, R. *J. Phys. Chem. A* **2003**, *107*, 11049.

(9) Becerra, R.; Goldberg, N.; Cannady, J. P.; Almond, M. J.; Ogden, J. S.; Walsh, R. *J. Am. Chem. Soc.* **2004**, *126*, 6816.

(10) Becerra, R.; Cannady, J. P.; Walsh, R. *J. Phys. Chem. A* **2004**, *108*, 3987.

(11) Chu, J. O.; Beach, D. B.; Estes, R. D.; Jasinski, J. M. *Chem. Phys. Lett.* **1988**, *143*, 135.

(12) Longeway, P. A.; Estes, R. D.; Weakliem, H. A. *J. Phys. Chem.* **1984**, *88*, 73.

(13) Dohmaru, T.; Lampe, F. W. *J. Photochem. Photobiol. A* **1987**, *41*, 275.

(14) Fikri, M.; Meyer, S.; Roggenbuck, S.; Temps, F. *Faraday Discuss.* **2001**, *119*, 223.

(15) Blitz, M. A.; Choi, N.; Kovacs, T.; Seakins, P. W.; Pilling, M. J. *Proc Combust. Symp.*, in press.

(16) Goldberg, N.; Ogden, J. S.; Almond, M. J.; Walsh, R.; Cannady, J. P.; Becerra, R.; Lee, J. A. *Phys. Chem. Chem. Phys.* **2003**, *5*, 5371.

(17) Becerra, R.; Frey, H. M.; Mason, B. P.; Walsh, R.; Gordon, M. S. *J. Chem. Soc., Faraday Trans.* **1995**, *91*, 2723.

(18) Baggott, J. E.; Frey, H. M.; King, K. D.; Lightfoot, P. D.; Walsh, R.; Watts, I. M. *J. Phys. Chem.* **1988**, *92*, 4025.

(19) Jasinski, J. M.; Chu, J. O. *J. Chem. Phys.* **1988**, *88*, 1678.

(20) Frisch, M. J.; Trucks, G. W.; Schlegel, H. B.; Scuseria, G. E.; Robb, M. A.; Cheeseman, J. R.; Zakrzewski, V. G.; Montgomery, J. A., Jr.; Stratmann, R. E.; Burant, J. C.; Dapprich, S.; Millam, J. M.; Daniels, A. D.; Kudin, K. N.; Strain, M. C.; Farkas, O.; Tomasi, J.; Barone, V.; Cossi, M.; Cammi, R.; Mennucci, B.; Pomelli, C.; Adamo, C.; Clifford, S.; Ochterski, J.; Petersson, G. A.; Ayala, P. Y.; Cui, Q.; Morokuma, K.; Malick, D. K.; Rabuck, A. D.; Raghavachari, K.; Foresman, J. B.; Cioslowski, J.; Ortiz, J. V.; Baboul, A. G.; Stefanov, B. B.; Liu, G.; Liashenko, A.; Piskorz, P.; Komaromi, I.; Gomperts, R.; Martin, R. L.; Fox, D. J.; Keith, T.; Al-Laham, M. A.; Peng, C. Y.; Nanayakkara, A.; Gonzales, C.; Challacombe, M.; Gill, P. M. W.; Johnson, B. G.; Chen, W.; Wong, M. W.; Andres, J. L.; Head-Gordon, M.; Replogle, E. S.; Pople, J. A. *Gaussian 98*, Revision A.9; Gaussian Inc.: Pittsburgh, PA, 1998.

(21) Curtiss, L. A.; Raghavachari, K.; Redfern, P. C.; Rassolov, V.; Pople, J. A. *J. Chem. Phys.* **1998**, *109*, 7764.

(22) Gonzales, C.; Schlegel, H. B. *J. Chem. Phys.* **1989**, *90*, 2154.

(23) Pople, J. A.; Scott, A. P.; Wong, M. W.; Radom, L. *Isr. J. Chem.* **1993**, *33*, 345.

(24) Holbrook, K. A.; Pilling, M. J.; Robertson, S. H. *Unimolecular Reactions*, 2nd ed.; Wiley: Chichester, 1996.

(25) Becerra, R.; Boganov, S.; Egorov, M. P.; Faustov, V. I.; Promyslov, V. M.; Nefedov, O. M.; Walsh, R. *Phys. Chem. Chem. Phys.* **2002**, *4*, 5079.

(26) Becerra, R.; Boganov, S.; Egorov, M. P.; Faustov, V. I.; Krylova, I. V.; Nefedov, O. M.; Promyslov, V. M.; Walsh, R. *Phys. Chem. Chem. Phys.* **2004**, *6*, 3370.

(27) Becerra, R.; Walsh, R. *Int. J. Chem. Kinet.* **1994**, *26*, 45.

(28) Al-Rubaiey, N.; Walsh, R. *J. Phys. Chem.* **1994**, *98*, 5303.

(29) Al-Rubaiey, N.; Carpenter, I. W.; Walsh, R.; Becerra, R.; Gordon, M. S. *J. Phys. Chem. A* **1998**, *102*, 8564.

(30) Becerra, R.; Boganov, S.; Walsh, R. *J. Chem. Soc., Faraday Trans.* **1998**, *94*, 3569.

(31) Becerra, R.; Cannady, J. P.; Walsh, R. *J. Phys. Chem. A* **1999**, *103*, 4457.

(32) Becerra, R.; Cannady, J. P.; Walsh, R. *Phys. Chem. Chem. Phys.* **2001**, *3*, 2343.

(33) Hippler, H.; Troe, J. In *Advances in Gas-Phase Photochemistry and Kinetics*; Ashfold, M. N. R., Baggott, J. E., Eds.; Royal Society of Chemistry: London, 1989; Vol. 2, Chapter 5, p 209.

(34) Sandhu, V.; Safarik, I.; Strausz, O. P.; Bell, T. N. *Res. Chem. Int.* **1989**, *11*, 19.

(35) Safarik, I.; Sandhu, V.; Lown, E. M.; Strausz, O. P.; Bell, T. N. *Res. Chem. Int.* **1990**, *14*, 105.

(36) Becerra, R.; Frey, H. M.; Mason, B. P.; Walsh, R. *J. Organomet. Chem.* **1996**, *521*, 343.

(37) Al-Rubaiey, N.; Becerra, R.; Walsh, R. *Phys. Chem. Chem. Phys.* **2002**, *4*, 5072.

(38) Benson, S. W. *Thermochemical Kinetics*, 2nd ed.; Wiley: New York, 1976.

(39) Troe, J. *J. Chem. Phys.* **1977**, *66*, 4758.

(40) Reid, R. C.; Prausnitz, J. M.; Poling, B. E. *The Properties of Gases and Liquids*, 4th ed.; McGraw-Hill: New York, 1988.

(41) Shapley, W. A.; Bacskay, G. B. *J. Phys. Chem. A* **1999**, *103*, 4505.

(42) Shapley, W. A.; Bacskay, G. B. *J. Phys. Chem. A* **1999**, *103*, 4514.

(43) Su, H.; Kong, F.; Chen, B.; Huang, M.-B.; Liu, Y. *J. Chem. Phys.* **2000.** *113*, 1885.